A Full-Wave High-Temperature Superconducting Rectifier Based on AC Field-Controlled Switches

Gengyao Li, Chao Li, Ying Xin, *Senior Member, IEEE*, and Bin Li, *Senior Member, IEEE*

***Abstract*—Due to the excellent properties, high-temperature superconducting (HTS) magnets are promising in high-intensity magnetic field applications. However, HTS magnets face a long-standing challenge of field decay due to connecting joint resistance and flux creep in superconductors. In this article, a novel full-wave HTS rectifier based on ac field-controlled switches is proposed to charge closed HTS magnets inductively. With advantages of compact structure, low cost and low heat load, the proposed full-wave HTS rectifier is capable of replacing the bulky dc power supply and thick current leads, which are required for maintaining the field stability of HTS magnets. An experimental prototype has been developed to verify its working principle. Tests have been carried out to illustrate parameters impacting the working characteristics. The proposed HTS rectifier can expand application scenarios and reduce the costs of HTS magnet significantly.**

***Index Terms*—Charging, high-temperature superconductor (HTS), rectifier, superconducting magnets, switches.**

I. Introduction

SUPERCONDUCTING magnets can generate high magnetic fields with very low energy consumption, thus laying the foundation for high-field applications such as nuclear fusion [1], high-power motors/generators [2], electron accelerators [3] and magnetic resonance imaging (MRI) [4]. High-temperature superconducting (HTS) materials have higher critical temperature, larger critical current density and higher critical magnetic field intensity than low-temperature superconducting (LTS) materials [5]. Hence, compared with LTS magnets, much higher magnetic fields can be achieved by HTS magnets. For example, the reported highest dc magnetic field is 45.5 T so far, which is achieved by combining a 14.4 T no-insulation HTS magnet as an insert magnet with a 31.1 T resistive background magnet [6].

However, HTS magnets still face many challenges, among which charging methods and magnetic field stability maintenance are major technical bottlenecks, limiting the development of HTS magnets [7]. The conventional method of charging the HTS magnet requires a high-capacity dc power supply and a pair of thick current leads from room temperature to cryogenic environment. This charging method leads to the following problems. Firstly, the high-capacity dc power supply requires an extremely high performance, resulting in exorbitant cost and huge volume. For example, the 50-kA power supply is used to charge the 20.1 T toroidal field magnet for the net-energy fusion tokamak developed by MIT [8]. The dc power supply consists of eight cabinets, which should be water-cooled [9]. Second, the current leads usually have a complex structure and cause relatively high heat leakage loss, which increases the cooling burden of cryogenic system and limits the current-carrying capability and energy density of the superconducting magnet [10]. Moreover, this heat ingress also reduces the thermal stability and reliability of the magnet [11]. Finally, the magnetic field stability of the dc superconducting magnet cannot be maintained when the HTS magnet operates in the persistent current mode. The persistent current mode means a magnetized superconducting magnet is operated in a closed loop circuit, which is fully formed by superconductors without external dc power supply. Unlike LTS magnets, superconducting joints between HTS tapes are still not available, thus causing joule heat loss generated by joint resistance in HTS magnets [12]. Besides, due to the characteristics of HTS materials, the flux creep occurring in HTS magnets is inevitable. These losses will cause continuous current decay in HTS magnets, weakening magnetic fields of HTS magnets.

To cope with above problems, it is very desirable to find a contactless charging method, which can eliminate the current leads from the magnet system, and instead to charge HTS magnets operated in closed-loop mode within a closed cryogenic environment. One possible solution is to employ a cryogenic rectifier located within the cryostat [13], [14]. A cryogenic rectifier can rectify the induced high alternating current in a closed cryogenic circuit by diodes, MOSFETs, or other semiconducting electronic components. However, the on-state resistance of semiconducting electronic components is too high so that much loss produced by rectifiers. The loss generated by rectifiers is a significant heat burden for cryogenic system and causes rapid current decay in closed superconducting magnets. Besides, it is difficult for power electronic components to achieve tens or even hundreds of kiloamps of dc current output.

Another alternative solution is to employ an HTS rectifier based on superconducting switches, which can inductively inject dc current into closed HTS magnets within a closed cryogenic environment [15]. The ac field-controlled switch relies on the transitions of the superconductor between the superconducting state (zero-resistance state) and the normal state. Hence,

Received 14 January 2024; revised 7 April 2024 and 24 June 2024; accepted 24 August 2024. Date of publication 30 August 2024; date of current version 7 October 2024. This work was supported in part by the National Natural Science Foundation of China under Grant 52107022. Recommended for publication by Associate Editor C. Fernandez. *(Corresponding author: Chao Li.)*

The authors are with the School of Electrical and Information Engineering, Tianjin University, Tianjin 300072, China. (e-mail: li_gengyao@tju.edu.cn; chaoli315@tju.edu.cn; yingxin@tju.edu.cn; binli@tju.edu.cn).

Color versions of one or more figures in this article are available at https://doi.org/10.1109/TPEL.2024.3452500.

Digital Object Identifier 10.1109/TPEL.2024.3452500

different from semiconducting electronic components, no extra heat loss is generated during the on-state of the HTS switch. Moreover, due to the high current carrying capacity of superconducting materials, the HTS rectifier can easily achieve a high current output. Therefore, due to the low loss and high current output, the HTS rectifier fits to charge the closed HTS magnet safely and efficiently in a contactless way. Geng and Coombs [16] proposed the mechanism of the HTS rectifier and verified the feasibility of the device. Geng et al. [17] and Zhou et al. [18] carried out investigations on working characteristics of HTS rectifiers. Li et al. [19], Gawith et al. [20], Li et al. [21], Geng et al. [22], and Rice et al. [23] researched ways to enhance the working performance of HTS rectifiers. Li et al. [24], Geng and Coombs [25], and Li et al. [26] proposed several modeling methodologies for HTS rectifiers, including the equivalent circuit and multi-physics coupling models. Brooks et al. [27], Jiang et al. [28], Wang and Coombs [29], and Li et al. [30] discussed the working principle and characteristics of field-controlled HTS switches.

However, all HTS rectifiers built in previous researches can only charge the HTS magnet in half cycles, which limits the charging speed and the efficiency. In this article, a novel full-wave HTS rectifier is proposed to charge the HTS magnet fast and efficiently. The novelty and contribution of the proposed method are as follows.

1) An HTS rectifier based on ac field-controlled switches is proposed to charge the closed dc HTS magnet using the ac power, thus saving the expensive high-capacity dc power supply and high-loss current leads. The proposed HTS rectifier is capable of charging the HTS magnet to the critical current.
2) The proposed HTS rectifier can charge the HTS magnet during the whole cycles. Thus, the charging speed and efficiency of the proposed full-wave HTS rectifier is at least one time larger than other existing HTS rectifiers.
3) An optimized topology of the proposed full-wave HTS rectifier is proposed to simplify the manufacturing process and save components. Based on the optimized topology, the proposed full-wave HTS rectifier achieves twice the performance at less than twice the cost of the half-wave HTS rectifier.

Moreover, experiments have been carried out to verify the proposed working principle and explore working characteristics of the proposed full-wave HTS rectifier.

The rest of this article is organized as follows. In Section II, the working principle of the proposed full-wave HTS rectifier based on field-controlled switches is introduced. In Section III, the experimental rig is described, including the full-wave HTS rectifier prototype and experimental apparatus for tests. In Section IV, experimental results are shown and analyzed. In Section V, the application scenarios of the proposed full-wave HTS rectifiers is discussed. Finally, Section VI concludes this article.

II. Working Principle of the Proposed HTS Rectifier

A. AC Field-Controlled HTS Switch

A superconducting switch should transfer between the zero resistance and the resistive state, thus allowing current to enter the closed superconducting circuit. The ac field-controlled HTS switch, which is used for achieving rectifying function, is composed of an electromagnet with a copper coil and an HTS tape, as shown in Fig. 1(a). The applied field strength refers to the ac magnetic field generated by the electromagnet and applied to the surface of an HTS tape. From the perspective of electrical circuit, when the ac field is applied, a dc voltage is induced across the HTS tape. This dc voltage can be used to charge the HTS magnet. When the ac field is removed, the dc voltage is disappeared. Then, the HTS magnet is operated in the persistent current mode. The HTS switch works based on the dynamic resistance. From a macroperspective, the above resistance will appear across an HTS tape carrying a direct transport current when a perpendicular alternating magnetic field is applied. During this process, no quench occurs in the HTS tape, which allows the resistance to disappear as soon as the applied alternating magnetic field is removed.

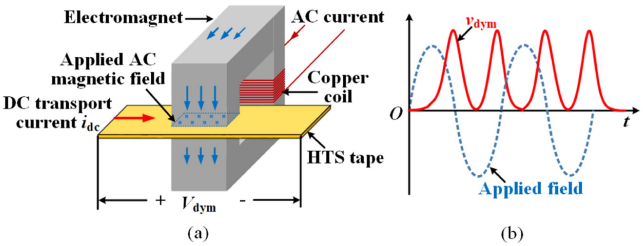

Fig. 1. Schematic drawing showing the working principle of the AC filed-controlled HTS switch used for the HTS rectifier. (a) Perpendicular ac magnetic field produced by an electromagnet is applied to the HTS tape carrying a direct transport current $i_{\rm dc}$, inducing a DC voltage $v_{\rm dym}$ across the HTS tape. (b) Instantaneous voltage $v_{\rm dym}$ across the HTS switch corresponding to the applied AC magnetic field.

From a microscopic perspective, the pinning force of HTS materials can be broke by the applied external ac magnetic field. Thus, a net magnetic flux flow across the HTS tape from one edge to the other is caused, through redistributing the vortices. The redistribution of the vortices interacts with the direct transport current in the HTS tape, which produces the dynamic resistance. The dynamic resistance can be calculated by

$$R_{\rm dym} = \frac{2alf}{I_c}(B_a - B_{a,\rm th}) \tag{1}$$

where I_c is the critical current of the HTS tape, a is the width of the HTS tape, l is the length of the HTS tape under the applied ac magnetic field, f is the frequency of the applied magnetic field, B_a is the amplitude of the applied flux density and $B_{a,\rm th}$ is the threshold flux density [31].

It should be noted that if the applied magnetic field is large enough, a sufficient dynamic resistance will be generated in the HTS switch, which can be served as the OFF-switching resistance to shut off a superconducting circuit. Correspondingly, the HTS switch has two working states, including the "ON" state and the "OFF" state. During the "ON" state, no current is applied to the copper coil of the electromagnet. Hence, the HTS switch has a zero resistance in this case that the direct current flows through in the HTS tape free from the external ac magnetic field. During the "OFF" state, an alternating current is powered to the copper coil of the electromagnet to produce a perpendicular ac magnetic field

to the surface of the HTS tape. As a result, a dynamic resistance is generated in the HTS switch.

In general, the HTS switch is used for charging the closed HTS magnet. Hence, the voltage across the HTS switch has significant impacts on the charging speed. For the ac field-controlled HTS switch, its average voltage $V_{\rm dym}$ can be described by

$$V_{\rm dym} = \frac{2i_{\rm dc}alf}{I_c}(B_a - B_{a,\rm th}) \tag{2}$$

where $i_{\rm dc}$ is the direct transport current in the HTS switch. It is noted the direction of $V_{\rm dym}$ is not determined by the direction of the applied magnetic field, but by the direction of current $i_{\rm dc}$ in the HTS switch. As long as the direction of $i_{\rm dc}$ does not change, the voltage generated across the HTS switch is a dc voltage. The red curve in Fig. 1(b) shows the schematic of instantaneous voltage $v_{\rm dym}$ induced across the HTS switch, which has two peaks per cycle of the applied ac magnetic field. Besides, it can be seen from (2) that $V_{\rm dym}$ is positively related with the amplitude and frequency of applied magnetic field as well as the direct transport current. Hence, the voltage across the HTS switch can be flexibly controlled.

Theoretically, according to (2), the higher applied ac fields strength, the higher dc voltage induced across the HTS tape. Correspondingly, the charging speed of the proposed rectifier is higher. However, the applied ac field strength should also be lower than the critical field strength of the HTS tape. Otherwise, the HTS tape will quench. Under the circumstance, even if the ac filed is removed, the resistance of HTS tape will still remain. This will cause the load current decay in the HTS magnet. It is suggested that the applied ac field strength should be lower than 500 mT according to electro-magnetic characteristics of existing HTS tapes.

The "ON" and "OFF" states of the proposed HTS switch are controlled by applying ac field. When the ac field is applied, the HTS switch is in the "OFF" state. When the ac field is removed, the HTS switch is in the "ON" state. Therefore, the switching frequency depends on the frequency of the applied ac field. The theoretical maximum switching frequency is several kilohertz. However, it should be noted that the high switching frequency is not necessary for the proposed HTS rectifier. This is because there is no other inductance or capacity in the circuit except for the load HTS magnet. Besides, the HTS magnet has no requirement for the smoothness of the charging current.

B. Proposed Full-Wave HTS Rectifier

The circuit diagram of the proposed full-wave HTS rectifier is shown in Fig. 2(a) and (b). The rectifier consists of a transformer and two HTS switches. In the transformer, primary windings and secondary windings are wound by copper wires and HTS tapes, respectively. It is recommended that the transformer has a high ratio n, so that high current can be induced in secondary windings by merely applying a low current $i_{\rm p}$ in primary windings. The two secondary windings a and b have opposite coupling directions with primary windings. Hence, the induced alternating currents in the two secondary windings have a phase difference of 180°. Two ac field-controlled HTS switches S_1 and S_2 are connected to secondary windings a and b, which forms two superconducting subloop circuits.

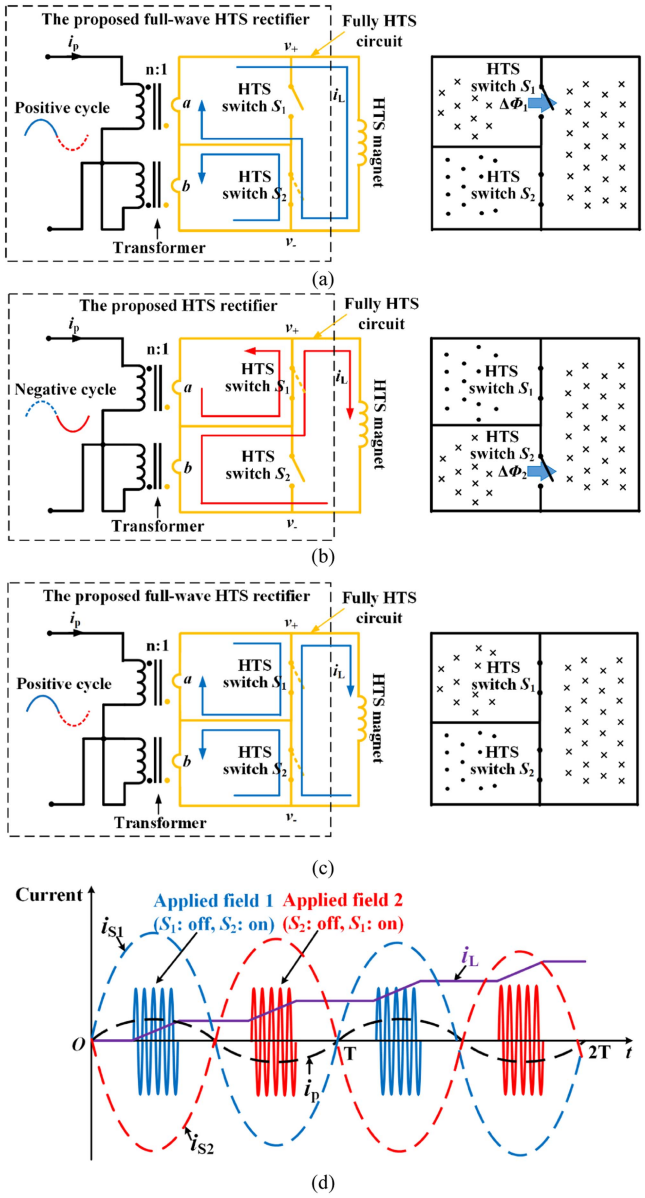

Fig. 2. Working principle of the proposed full-wave HTS rectifier based on ac field-controlled HTS switches. (a) During the positive cycle, the HTS switch S_1 is in the "OFF" state, whereas the HTS switch S_2 is in the "ON" state. The current is shown in blue. (b) During the negative cycle, the HTS switch S_2 is in the "OFF" state, whereas the HTS switch S_1 is in the "ON" state. The current is shown in red. During the whole cycle, the DC voltage on two switches is in the same direction, so that the magnetic flux is continually injected into the HTS magnet. (c) Current path and equivalent circuit in the persistent current mode. (d) Working performance of the proposed HTS rectifier.

The working states of the proposed full-wave HTS rectifier can be classified into two modes, namely, the persistent current mode and the charging mode, which are determined by the HTS switches triggered by the applied field.

In the persistent current mode shown in Fig. 2(c), no ac magnetic field is applied to S_1 and S_2, so that S_1 and S_2 are both in the "ON" state. Due to the zero resistance of superconductors, the HTS magnet is short-circuited by S_1 and S_2. The output voltage

of the rectifier is zero. Hence, alternating current in secondary windings cannot flow into the HTS magnet. Hence, the current in the HTS magnet maintains a constant, except for the loss caused by the joint resistance.

In the charging mode, the high-frequency ac magnetic field is intermittently applied on S_1 and S_2, so that two switches are turned on alternately per cycle. Since the direction of current in HTS switches is always the same at each time the magnetic field is applied, the load current i_{L} in the HTS magnet can be accumulated step by step. The working performance of the proposed HTS rectifier is shown in Fig. 2(d).

To be specific, during the positive cycle of the primary winding current, S_1 is in the "OFF" state, whereas S_2 is in the "ON" state at the same time, as shown in Fig. 2(a). Since the current in the subloop circuit including S_1 is clockwise (shown in blue), the induced voltage across S_1 is downward. Thus, the HTS magnet is charged by the voltage of S_1, generating a downward current in it. From the perspective of flux, the magnetic flux $\Delta\Phi_1$ increased in the HTS magnet per positive cycle can be expressed by

$$\Delta\Phi_1 = V_{\mathrm{dym1}}T \tag{3}$$

where V_{dym1} is the average voltage across S_1 and T is the cycle of the primary winding current.

The working process during the negative cycle of the primary winding current is similar with that during the positive cycle. During the negative cycle, S_2 is in the "OFF" state, whereas S_1 is in the "ON" state at the same time, as shown in Fig. 2(b). Since the current in the subloop circuit including S_2 is clockwise (shown in red), the induced voltage on S_2 is downward. The magnetic flux $\Delta\Phi_2$ increased in the HTS magnet per negative cycle can be expressed by

$$\Delta\Phi_2 = V_{\mathrm{dym2}}T \tag{4}$$

where V_{dym2} is the average voltage across S_2.

Overall, during the whole cycle, a downward output voltage is generated by the full-wave HTS rectifier, thus the HTS magnet is charged continuously. The increased current in the HTS magnet per cycle is

$$\Delta i_{\mathrm{L}} = \frac{\Delta\Phi_1 + \Delta\Phi_2}{L} \tag{5}$$

where L is the inductance of the HTS magnet.

III. Experimental System

A. Optimized Circuit Topology of the Proposed Full-Wave HTS Rectifier

Based on the proposed working principle, the full-wave HTS rectifier is further optimized during the process of building the prototype. Only one iron core for the transformer is used in the optimized rectifier prototype, whose specific circuit topology is shown in Fig. 3. The transformer is used to supply high transport currents for two HTS switches. Electromagnet 1 and electromagnet 2 are used to apply ac fields on HTS tapes.

The design and optimization procedure the transformer is as follows.

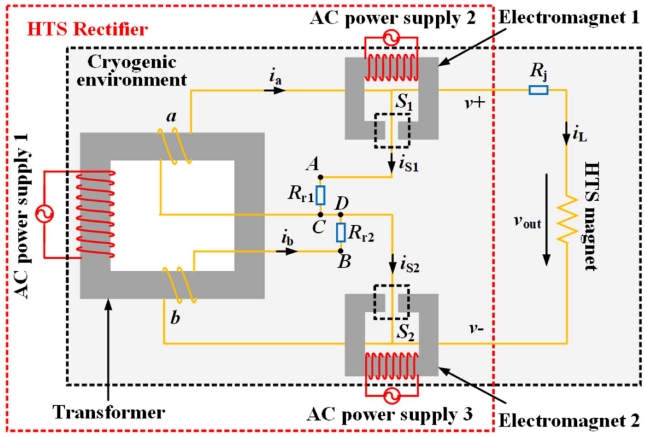

Fig. 3. Optimized circuit topology of the proposed full-wave HTS rectifier.

First, determine the maximum secondary winding current I_{sm}. In order to ensure that the proposed HTS rectifier can charge the HTS magnet to its maximum operating current I_{Lm} it is suggested that

$$I_{\mathrm{sm}} > 1.5I_{\mathrm{Lm}}. \tag{6}$$

Second, determine the transformer ratio n. If the ac current source can supply the maximum current I_{pm} for the primary winding, the transformer ratio n can be calculated by

$$n = \frac{I_{\mathrm{sm}}}{I_{\mathrm{pm}}}. \tag{7}$$

Third, determine the turns of the primary and secondary windings according the transformer ratio n. In order to avoid reducing the critical current of HTS tapes, the turns of the secondary windings are set to be 1 or 2. Correspondingly, the turns of the primary winding turn N_p are set to be $2n$ or $4n$.

Finally, determine the size of the iron core. In order to keep the safe operation of the proposed HTS rectifier, the iron core should be maintained unsaturated when the primary current achieves the maximum current I_{pm}. According to the magnetic hysteresis loop of the iron core material, the saturation magnetization field H_m and saturation flux density B_m can be determined. According to Ampere's circulation theorem, the length l_{t} and the cross-sectional area S_{t} of the iron core can be calculated by

$$\begin{cases} l_t = \frac{H_m}{N_p I_{\mathrm{pm}}} \\ S_t = \frac{B_m}{L I_{\mathrm{pm}}} \end{cases} \tag{8}$$

where N_p is the turn number of the primary winding, and L is the inductance of the primary winding.

The design and optimization procedure of electromagnet 1 and electromagnet 2 is as follows.

Firstly, determine the maximum applied field B_a, according to the voltage V_{dym} of HTS switch. It can be calculated by

$$V_{\mathrm{dym}} = \frac{2i_{\mathrm{dc}}alf}{I_c}(B_a - B_{a,\mathrm{th}}). \tag{9}$$

Second, determine the material of iron core according to the maximum applied field B_a. The material should be maintained unsaturated under the magnetic field B_a.

Third, determine the cross-sectional area of the iron core. The length of cross section equals the length of HTS tape under the applied ac field.

Finally, determine the total length l_m of magnetic circuit and the turn N_c of copper coil. According to Ampere's circulation theorem, it can be calculated by

$$N_c I_{\mathrm{em}} = B_a \left(\frac{l_a}{\mu_0} + \frac{l_m}{\mu_e \mu_0} \right) \tag{10}$$

where I_{em} is the maximum current of the copper coil, l_m is the length of the air gap, μ_e is the relative permeability of the iron core, and μ_0 is the permeability of vacuum.

In order to reduce the required cooling power, volumes of the transformer and electromagnets should be minimized as much as possible. In order to reduce the loss caused by leakage inductance, secondary windings can be coupled tightly to the iron core. Besides, to reduce the heat load of the cryogenic system, the copper winding and the iron core can be placed outside the cryogenic container.

It should be noted that the method to wind the HTS tape around the closed iron core really does matter. The steps of manufacturing the secondary circuit should be as follows: First, threading the tape through the hole of the transformer iron core, where terminals *A* and *B* are ends of the tape. Second, clockwise wounding one half of the tape twice around on side of the iron core and clockwise wounding the other half of the tape twice around on the other side of the iron core. Then, choosing two points *C* and *D* on the tape, which should stagger a distance. Finally, soldering the tape terminal *A* to the point *C* forming a solder resistance R_{r1} and soldering the tape terminal *B* to the point *D* forming a solder resistance $R_{\mathrm{r}2}$, thus a closed superconducting circuit is built.

The above manufacturing method has many benefits. First, it allows the inner resistance of the rectifier is zero, thus avoiding unnecessary joule heat loss. Second, it simplifies the manufacturing process. Only two solder joints are needed to make a circuit where two closed windings are connected. Thirdly, the staggered distance *CD* ensures the HTS tape of two secondary subloop circuits not overlapped, preventing current in HTS tape from exceeding the critical current.

B. Full-Wave HTS Rectifier Prototype

A full-wave HTS rectifier prototype using ac field-controlled HTS switches has been built corresponding to the above circuit topology, as shown in Fig. 4. The primary winding of the transformer is made of a 200-turn copper winding, which is wound around a closed iron core. Secondary windings *a* and *b* are composed of two 2-turn HTS coils, which are wound clockwise around two opposite sides of the iron core respectively. It is noted that the whole secondary circuit is manufactured by a single HTS tape, where terminals of two secondary windings are welded together using two solder joints. 4 mm wide and 0.2 mm thick Bi-2223 tapes manufactured by Sumitomo Corporation is used for the secondary circuit, and it has a critical current I_c of 180 A at 77 K. The threshold flux density $B_{a,\mathrm{th}}$ of the HTS tape is 20 mT. In each subloop circuit, a 60 mm long tape is combined with an electromagnet to form an HTS switch. Each electromagnet has a copper winding of 100 turns and an air gap of 3 mm, which allows it to generate a magnetic field larger than 200 mT. The output terminals are marked with v_+ and v_-, where the load HTS magnet can be connected to obtain a dc excitation voltage.

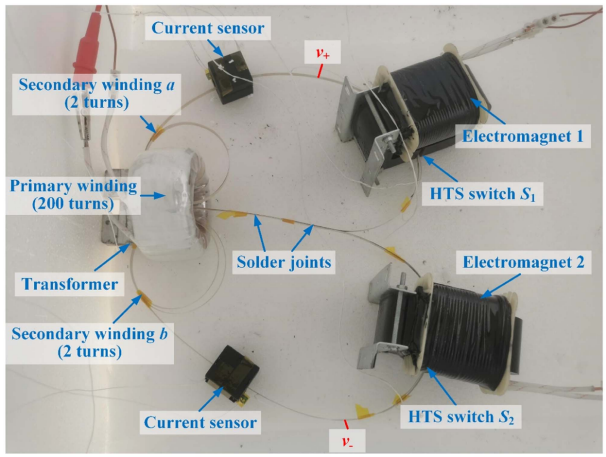

Fig. 4. Photo of the experimental prototype of the proposed full-wave HTS rectifier.

When an alternating current is applied to the primary winding, the current i_{a} in secondary winding *a* and the current i_b in secondary winding *b* have a phase difference of 180°. The current i_{S1} in S_1 and the current i_{S2} in S_2 are always in the opposite direction. Hence, a dc voltage $\mathrm{v_{out}}$ on the output terminals of the rectifier can be generated by alternately applying an ac magnetic field to S_1 and S_2 during positive cycles and negative cycles. It is noted that all excitations are realized by electromagnetic coupling in a fully superconducting circuit located in a cryogenic environment, so that the conventional electrical contact to the HTS magnet through thick superconducting current leads is avoided. Therefore, the rectifier is capable of energizing the HTS magnet wirelessly in a closed cryogenic environment, which guarantees the safe and steady operation of HTS magnets.

C. Experimental Apparatus for Testing the HTS Rectifier

An HTS magnet wound by 4 mm wide Bi-2223 tape with 56 turns is used for the load of the HTS rectifier, as shown in Fig. 5. The HTS magnet has an inner diameter of 60 mm and an outer diameter of 75 mm. The inductance of the HTS magnet is measured to be 300 μH. When performing a load test on the rectifier, the HTS magnet is soldered to the output terminals of the rectifier. Specifications of the HTS magnet are given in Table I.

Fig. 6 shows the experimental rig for testing the working performance of the proposed HTS rectifier. The primary winding of the transformer is powered by an amplifier ATA-3090 with an output power of 10 W (ac power supply 1 in Fig. 3). The electromagnets for HTS switches are powered by a Crown T10 dual-channel amplifier with an output power of 5 W (ac power supply 2 and ac power supply 3 in Fig. 3). Signals of these two

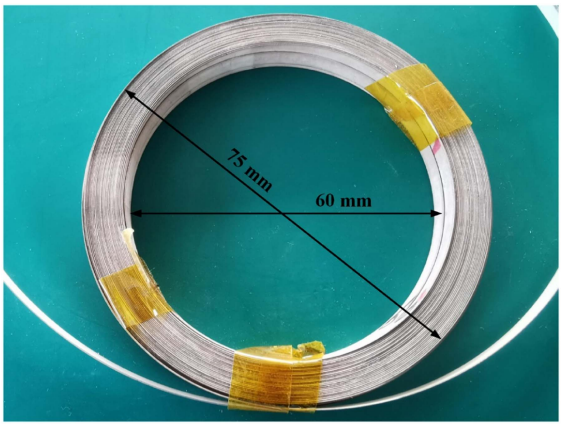

Fig. 5. Photo of the Bi-2223 HTS magnet used for the load of the proposed HTS rectifier.

TABLE I
SPECIFICATIONS OF THE HTS MAGNET

Parameters	Specifications
Material	Bi-2223
Shape	Double pancake
Critical current	110 A at 77 K
Turn numbers	56
Inner diameter	60 mm
Outer diameter	75 mm
Height	10 mm
Self-inductance	300 μH

amplifiers is given by a multichannel signal generator, which is driven by a computer with a controlling software. A 0.1 Ω standard resistance with voltage leads soldered to both ends is connected in series to each output terminal of amplifiers. Hence, current in the primary winding, electromagnet 1 and electromagnet 2 can be measured.

Current sensors shown in Fig. 4 are used for measuring the current in the prototype. A current sensor is made of a hall sensor and an iron core with an air gap. A high-precision dc constant current supply is used to power hall sensors. Through calibrating the current sensor under known current, the current sensor can measure the current accurately. Three current sensors are made to measure current in secondary winding *a*, secondary winding *b* and the HTS magnet. At output terminals of the rectifier, two voltage leads twisted together are soldered to measure the instantaneous output voltage of the HTS rectifier. All measured signals are collected by a NI data acquisition system driven by the LabVIEW program with a sample frequency of 5000 Hz. The HTS rectifier prototype is placed in a polystyrene foam box, which is infused with liquid nitrogen to provide a cryogenic environment of 77 K.

D. Control Method of the HTS Rectifier

Fig. 7 shows the control flow chart of the proposed full-wave HTS rectifier. The detailed control flow is described as follows.

First, turn ON the ac power supply to apply a low-frequency alternating current to the primary winding of the transformer.

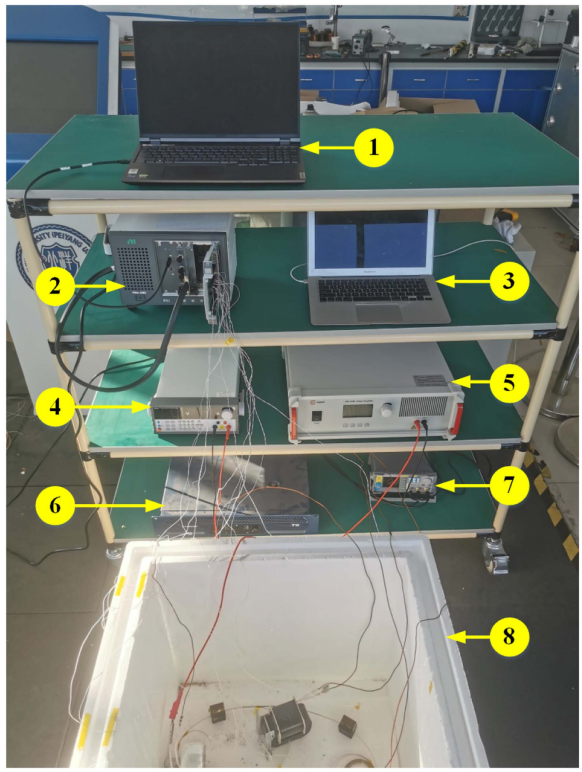

Fig. 6. Experimental system for testing the proposed HTS rectifier. (1) Computer used for data acquisition. (2) NI data acquisition system. (3) Computer used for controlling the multichannel signal generator. (4) High-precision dc constant current supply for current sensors. (5) ATA-3090 amplifier for powering the transformer. (6) Crown T10 dual-channel amplifier for powering electromagnets in HTS switches. (7) Multichannel signal generator for providing signal waveforms to power amplifiers. (8) HTS rectifier prototype in a polystyrene foam box.

Second, detect secondary winding currents to judge which half cycle the secondary winding currents are during. Third, if secondary winding currents are during positive cycles, open the HTS switch S_1 and close the HTS switch S_2. If secondary winding currents are during negative cycles, close the HTS switch S_1 and open the HTS switch S_2. Fourth, detect the average output voltage $V_{\rm out}$ of the HTS rectifier, and compare it with the target output voltage $V_{\rm target}$ of the HTS rectifier. Fifth, if $V_{\rm out} < V_{\rm target}$, adjust the frequency/amplitude/duration of applied ac fields or the frequency/amplitude of the primary winding current to increase $V_{\rm out}$. Sixth, detect the load current i_L of the HTS magnet, and compare it with the target operating current $i_{\rm target}$ of the HTS magnet. Finally, if $i_L < i_{\rm target}$, continue opening two HTS switches alternatively. Otherwise, close two HTS switches to operate the HTS magnet in the persistent current mode.

At the beginning of charging HTS magnets, it is recommended to use a large duty cycle to obtain a high average output voltage. When the current in HTS magnet approaching the target operating current, the duty cycle should be reduced for a more precise control. Besides, it is better for the rectifier to be operated under a low frequency, which can reduce the ac loss generated in HTS coils. Meanwhile, the frequency cannot be too low, otherwise the transformer core may saturate during switching.

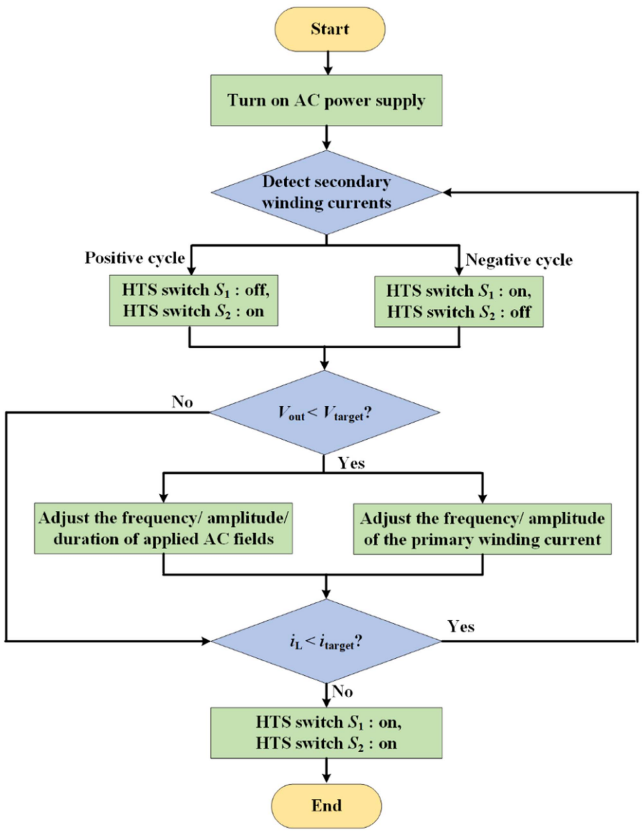

Fig. 7. Control flow chart of the proposed full-wave HTS rectifier.

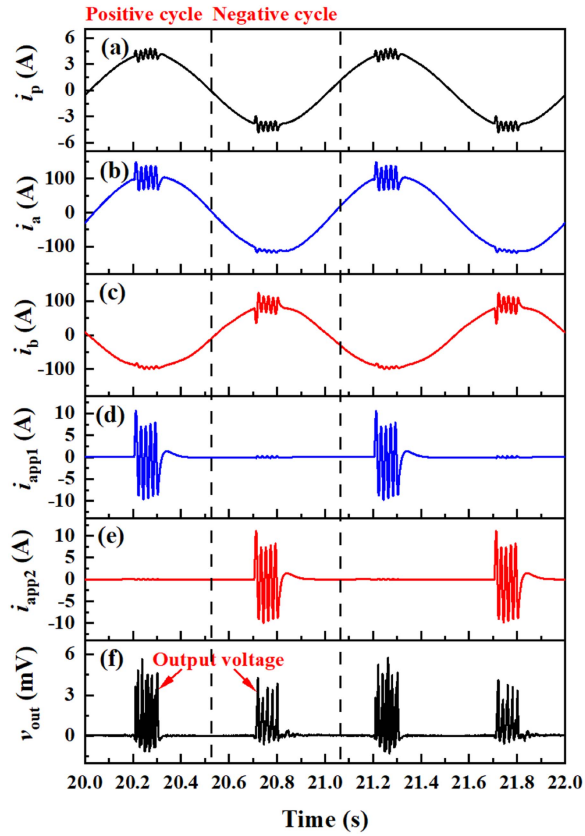

Fig. 8. Open-circuit test results of the proposed HTS rectifier. (a) Current of the transformer primary winding. (b) Current of the secondary winding *a*. (c) Current of the secondary winding *b*. (d) Current of the electromagnet 1. (e) Current of the electromagnet 2. (f) Output voltage of the HTS rectifier.

IV. Experimental Results and Analysis

A. Open-Circuit Test

Open-circuit tests of the proposed HTS rectifier were carried out in the condition that no load was connected to the output terminals of the rectifier. The primary winding of the transformer was powered by a sinusoidal current i_p with an amplitude of 4 A and a frequency of 1 Hz. Two electromagnets for applying magnetic fields in HTS switches S_1 and S_2 were powered by two sinusoidal currents i_{app1} and i_{app2}, each of which had an amplitude of 7.5 A and a frequency of 50 Hz. In this case, the magnetic field amplitude B_a generated by the electromagnet was measured to be 100 mT by a hall sensor. Currents i_{app1} and i_{app2} were respectively applied during the positive cycles and negative cycles of i_p, thus only one switch was turned on during each half cycle. Currents i_{app1} and i_{app2} were applied around peaks of i_p, and the duration of these currents was 0.1 s per cycle of i_p.

Fig. 8 shows open-circuit test results based on the above experimental conditions. It can be seen from Fig. 8(b) and (c) that the current i_{a} in secondary winding *a* and the current i_{b} in secondary winding *b* have a phase difference of 180°and both have the amplitudes of around 110 A under the excitation of the primary winding current i_p shown in Fig. 8(a). Fig. 8(d) and (e), respectively, shows currents i_{app1} and i_{app2} of intermittent applied magnetic fields.

Fig. 8(f) shows the instantaneous output voltage v_{out} of the rectifier. It can be observed as soon as an HTS switch is triggered, a dc voltage is generated across the output terminals, which has a peak of approximately 5 mV. The average voltage V_{dym} of the HTS switch is calculated to be 0.81 mV. The little negative value in the output voltage is due to the measurement noises caused by applied alternating magnetic field. By triggering two switches alternatively, the positive output voltage can be induced throughout one entire cycle. Hence, the average value of the output voltage is significantly enhanced through the full-wave rectification. Meanwhile, it should be noted that according to (2), the average voltage of each HTS switch can be adjusted by several ways, such as changing the amplitude or frequency of i_p, and changing the amplitude, frequency or duration of i_{app1} and i_{app2}.

B. Performance of Charging the HTS Magnet

In order to verify the charging performance, the proposed full-wave HTS rectifier was soldered to an HTS magnet. The soldered joint resistance was measured to be 1 $\mu\Omega$. In tests of charging the HTS magnet, the proposed HTS rectifier worked in the full-wave rectifying mode and the half-wave rectifying mode respectively. The parameters of i_p, i_{app1}, and i_{app2} were set to be same as those in open-circuit tests.

Fig. 9 shows experimentally charging performance of the proposed HTS rectifier, including current waveforms of the primary winding, applied ac fields, two HTS switches and the load HTS

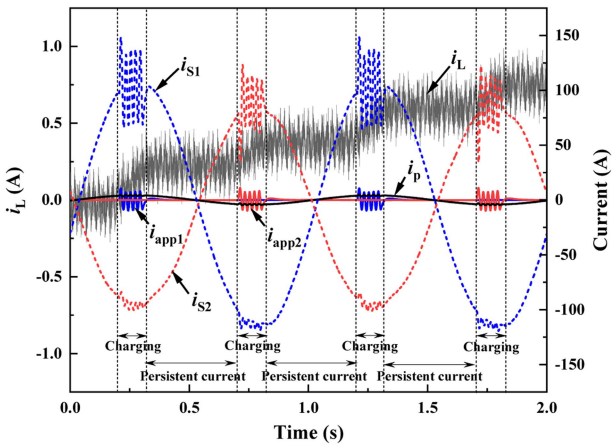

Fig. 9. Charging performance of the proposed HTS rectifier.

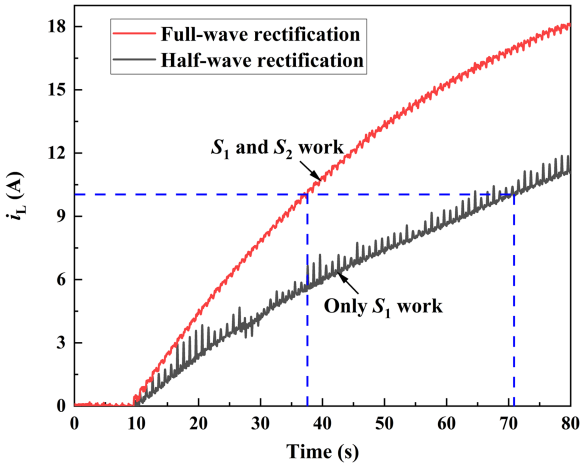

Fig. 10. Load current i_L of the HTS magnet in cases that the proposed HTS rectifier works in the full-wave rectifying mode and the half-wave rectifying mode.

magnet. The results are consistent with the working performance shown in Fig. 2(d), thus verifying the correctness of the proposed working principle.

Fig. 10 shows curves of the HTS magnet load current i_L, which have been dealt with a low-pass filter using a cutoff frequency of 5 Hz. From 0 to 10 s, the primary winding of the transformer was powered by ac power supply, but no HTS switch was triggered. Accordingly, the HTS magnet was not charged. Then, the proposed rectifier worked in the charging mode and the two switches were alternately triggered from 10 s. Correspondingly, the HTS magnet was charged. It can be seen that the load current in the HTS magnet reached 10 A after 28 s, verifying the correctness of the working principle of the proposed full-wave HTS rectifier. In contrast, if only the switch S_1 was triggered, i.e., the half-wave rectification, the load current in the HTS magnet reached 10 A after 61 s, which indicates the charging speed of the proposed HTS full-wave rectifier is at least one time larger than the existing HTS rectifiers. Hence, it demonstrates that the proposed full-wave rectifier based on the new circuit topology can improve the speed for charging the HTS magnet significantly.

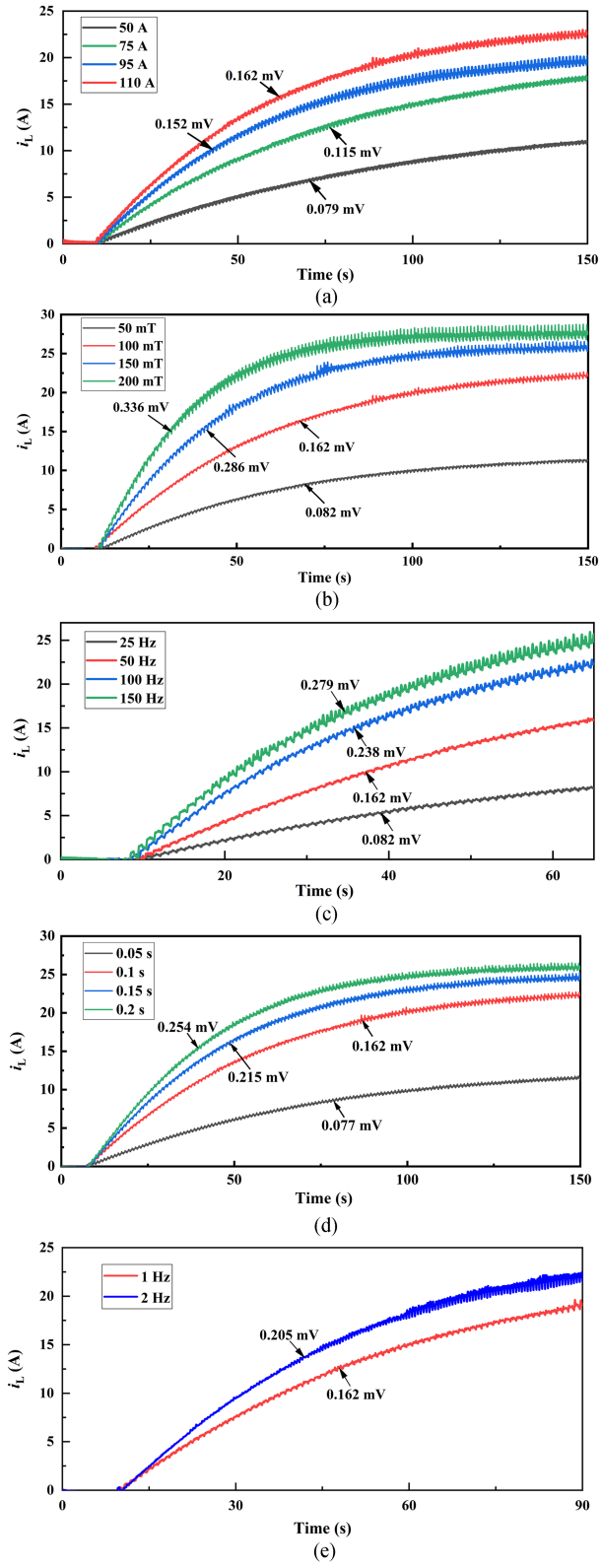

Fig. 11. Load current i_L of the HTS magnet and average voltage across the proposed HTS rectifier under different conditions. The rectifier served as the control group (red curve) has a secondary winding current amplitude i_{swm} of 110 A, an applied field amplitude B_{appm} of 100 mT, an applied field frequency f_{app} of 50 Hz, an applied field duration t_{app} of 0.1 s and a primary current frequency f_p of 1 Hz. (a) $i_{swm} = 50, 75, 95, 110$ A. (b) $i_{appm} = 50, 100, 150, 200$ mT. (c) $f_{app} = 25, 50, 100, 150$ Hz. (d) $t_{app} = 0.05, 0.1, 0.15, 0.2$ s. (e) $f_p = 1, 2$ Hz.

TABLE II
COMPARISON RESULTS WITH OTHER EXISTING WORK

	Proposed full-wave HTS rectifier	Half-wave HTS rectifier	Rectifier using semiconductor switches	Conventional charging method
Circuit	One transformer and two HTS switches	One transformer and one HTS switch	One transformer and two or four semiconductor switches	One high-capacity DC power supply and a pair of current leads
Charge closed HTS magnets	Yes	Yes	Yes	No
Efficiency	High	Medium	Medium	Low
Cost	Low	Low	Medium	High
Complexity	Low	Low	Low	High
Charging speed	Fast	Slow	Fast	Fast

Meanwhile, it is noted that with the increase of the accumulated load current in the HTS magnet, the charging speed becomes slower. This is because the gradual increase of the load current in the HTS magnet decreases the current in the HTS switches. In practical applications, the efficiency and effectiveness of the proposed HTS rectifier will be enhanced, when it is scaled up for larger HTS magnets. Larger HTS magnets need larger HTS switches, indicating more HTS tapes are applied to an ac magnetic field. Thus, the HTS rectifier can generate a larger output voltage. The proposed HTS rectifier is capable of charging HTS magnets to their critical current.

C. Working Characteristics of the Proposed Full-Wave Rectifier

To further explore the working characteristics of the full-wave HTS rectifier, tests under different operating conditions were carried out. In each set of these experiments, only one parameter of the rectifier was changed. The load current of the HTS magnet was measured, and the average voltage across the rectifier per cycle was calculated by

$$V_{\text{out}} = \frac{1}{T}\int_0^T v_{\text{out}} dt. \tag{11}$$

Fig. 11 shows load current of the HTS magnet and average voltage across the HTS rectifier under different operating parameters. It is clear the charging speed for the HTS magnet has been enhanced by increasing the amplitude i_{swm} of secondary winding current, or increasing the amplitude $i_{\text{app}m}$, frequency f_{app} or duration t_{app} of applied magnetic field. Meanwhile, Fig. 11(a), (b), and (c) shows that the average voltage across the rectifier is basically increased linearly with the increase of $i_{\text{sw}m}$, $i_{\text{app}m}$ or f_{app}. It should be noted that the direct transport current i_{dc} in (2) corresponds to the difference between the secondary winding current and the load current. Thus, the current in the switches during each cycle is not a constant. This is why the average voltage across the rectifier is not completely proportional to $i_{\text{sw}m}$ or $i_{\text{app}m}$. Fig. 11(d) shows that the extension of the applied magnetic field duration t_{app} can increase the average voltage. However, it is necessary to make sure the current in the HTS switch is positive when ac magnetic field is applied, otherwise the negative voltage will be generated across the switches, causing the reduction of the average output voltage across the rectifier. Fig. 11(e) shows that the charging speed can be enhanced by increasing the frequency f_p of the primary winding current. It is noted that the average voltage across the rectifier at 2 Hz did not increase to twice the average voltage across the rectifier at 1 Hz. This is because the effective current in HTS switches per cycle decreases with the increase of the primary current frequency.

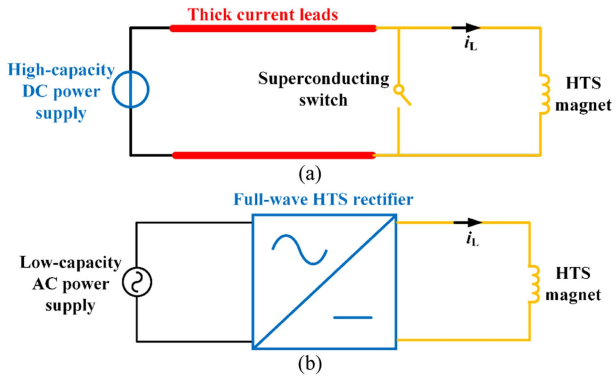

Fig. 12. Comparison between the different methods of charging the HTS magnet. (a) Circuit of the conventional method for directly charging the HTS magnet. (b) Circuit of charging the HTS magnet using proposed full-wave HTS rectifier.

V. DISCUSSION

The conventional method of charging the HTS magnet usually requires a bulky dc power supply and a pair of thick current leads, as shown in Fig. 12(a). These resistive current leads will generate a considerable heat load in the cryogenic system, limiting the operating current and adding the operating cost of HTS magnet. In contrast, the proposed full-wave HTS rectifier, combining with low-capacity ac power supply, can output dc voltage to charge the HTS magnet, as shown in Fig. 12(b). Since the energy transmission and the control of switches are both achieved by electromagnetic coupling, the direct electrical contact is avoided. In this way, the dc power supply and thick current leads can be replaced.

The proposed full-wave HTS rectifier can compensate the field decay of the HTS magnet in a smaller, lighter and cheaper

way. Hence, it is promising in many applications, such as MRI using HTS magnets and HTS wind generators. These HTS magnets are usually operated in the persistent current mode after they are charged to the target magnetic field. Due to the complex electromagnetic background they are placed in, field decay caused by power loss is unavoidable. Correspondingly, these large magnets generally need to be recharged after hours or days. In this case, the conventional method is not convenient for charging the HTS magnet so frequently. The proposed full-wave HTS rectifier can be controlled precisely, because the switches, controlled by ac field, are capable of switching "on" and "off" without any delay. Therefore, it can improve the working performance of the HTS magnets.

To further validate the effectiveness and superiority of the proposed full-wave HTS rectifier, other existing work is applied to make a comparison in different aspects, as given in Table II. It can be seen that the proposed full-wave HTS rectifier has good comprehensive performance.

VI. Conclusion

In this article, a novel full-wave HTS rectifier based on ac field-controlled switches is proposed to charge closed dc HTS magnets, which can avoid utilizing conventional bulky dc power supply and thick current leads. The conclusions can be drawn as follows.

First, the charging speed of the proposed full-wave HTS rectifier is at least one time larger than other existing HTS rectifiers, which improves the working performance significantly. Second, the proposed HTS rectifier relies on merely two field-controlled HTS switches to achieve full-wave rectification, which reduces the operating cost. Third, an optimized topology of the proposed full-wave HTS rectifier is proposed to simplify the manufacturing process and save the components. Finally, the charging voltage of the proposed full-wave HTS rectifier is basically proportional to the amplitude of the secondary winding current, the amplitude and frequency of the applied field, and positively related with the duration of the applied field and the frequency of the primary winding current. The proposed full-wave HTS rectifier is of significant in promoting the rapid development of HTS magnets.

References

[1] X. Deng, C. Wan, L. Jiang, G. Gao, and Y. Huang, "Open-switch fault diagnosis of three-phase PWM converter systems for magnet power supply on EAST," *IEEE Trans. Power Electron.*, vol. 38, no. 1, pp. 1064–1078, Jan. 2023.

[2] Q. Ge, B. Kou, H. Zhang, X. Du, and M. Wang, "Harmonic magnetic field analysis method and modeling of double-sided air-cored superconducting linear synchronous motor for EDS train," *IEEE Trans. Ind. Electron.*, vol. 70, no. 2, pp. 1717–1728, Feb. 2023.

[3] Y.-F. Liu, M. G. Gum, Q.-B. Yuan, R. Wang, J. Tong, and S. Li, "Development of a MHz pulsed power supply for kicker magnet in SHINE," *IEEE Trans. Power Electron.*, vol. 39, no. 4, pp. 4291–4300, Apr. 2024.

[4] J. Cheng et al., "Progress of the 9.4-T whole-body MRI superconducting coils manufacturing," *IEEE Trans. Appl. Supercond.*, vol. 28, no. 4, Jun. 2018, Art. no. 4402005.

[5] Y. Iwasa, "HTS magnets: Stability; protection; cryogenics; economics; current stability/protection activities at FBML," *Cryogenics*, vol. 43, no. 3–5, pp. 303–316, 2003.

[6] S. Hahn et al., "45.5-tesla direct-current magnetic field generated with a high-temperature superconducting magnet," *Nature*, vol. 570, no. 7762, pp. 496–499, Jun. 2019.

[7] T. A. Coombs, "Superconducting flux pumps," *J. Appl. Phys.*, vol. 125, no. 23, Jun. 2019, Art. no. 230902.

[8] Z. S. Hartwig et al., "The SPARC toroidal field model coil program," *IEEE Trans. Appl. Supercond.*, vol. 34, no. 2, Mar. 2024, Art. no. 0600316.

[9] T. Golfinopoulos et al., "Building the runway: A new superconducting magnet test facility made for the SPARC toroidal field model coil," *IEEE Trans. Appl. Supercond.*, vol. 34, no. 2, Mar. 2024, Art. no. 0600416.

[10] A. Ballarino et al., "Design of the HTS current leads for ITER," *IEEE Trans. Appl. Supercond.*, vol. 22, no. 3, Jun. 2012, Art. no. 4800304.

[11] C. Li et al., "Persistent current switch for HTS superconducting magnets: Design, control strategy, and test results," *IEEE Trans. Appl. Supercond.*, vol. 29, no. 2, Mar. 2019, Art. no. 4900704.

[12] C. Wu, W. Wang, R. Long, H. Li, L. Zhou, and P. Liu, "Fast current regulation and persistent current maintenance of high-temperature superconducting magnets with contact power supply and flux pump," *IEEE Trans. Power Electron.*, vol. 39, no. 4, pp. 4805–4814, Apr. 2024.

[13] Z. C. Zhang and B. T. Ooi, "Multimodular current-source SPWM converters for a superconducting magnetic energy storage system," *IEEE Trans. Power Electron.*, vol. 8, no. 3, pp. 250–256, Jul. 1993.

[14] W. Guo, D. Li, F. Cai, C. Zhao, and L. Xiao, "Z-source-converter-based power conditioning system for superconducting magnetic energy storage system," *IEEE Trans. Power Electron.*, vol. 34, no. 8, pp. 7863–7877, Aug. 2019.

[15] L. J. M. van de Klundert and H. H. J. ten Kate, "On fully superconducting rectifiers and fluxpumps. A review. Part 2: Commutation modes, characteristics and switches," *Cryogenics*, vol. 21, no. 5, pp. 267–277, May 1981.

[16] J. Geng and T. A. Coombs, "Mechanism of a high-Tc superconducting flux pump: Using alternating magnetic field to trigger flux flow," *Appl. Phys. Lett.*, vol. 107, no. 14, 2015.

[17] J. Geng, K. Matsuda, L. Fu, B. Shen, X. Zhang, and T. A. Coombs, "Operational research on a high-Tc rectifier-type superconducting flux pump," *Supercond. Sci. Technol.*, vol. 29, no. 3, 2016, Art. no. 035015.

[18] P. Zhou et al., "A contactless self-regulating HTS flux pump," *IEEE Trans. Appl. Supercond.*, vol. 30, no. 4, Jun. 2020, Art. no. 3603006.

[19] C. Li et al., "Design for a persistent current switch controlled by alternating current magnetic field," *IEEE Trans. Appl. Supercond.*, vol. 28, no. 4, Jun. 2018, Art. no. 4603205.

[20] J. D. D. Gawith et al., "A half-bridge HTS transformer–rectifier flux pump with two AC field-controlled switches," *Supercond. Sci. Technol.*, vol. 31, no. 8, 2018, Art. no. 085002.

[21] C. Li, J. Geng, B. Shen, J. Ma, J. Gawith, and T. A. Coombs, "Investigation on the transformer-rectifier flux pump for high field magnets," *IEEE Trans. Appl. Supercond.*, vol. 29, no. 5, Aug. 2019, Art. no. 4301105.

[22] J. Geng et al., "A kilo-ampere level HTS flux pump," *Supercond. Sci. Technol.*, vol. 32, no. 7, 2019, Art. no. 074004.

[23] J. H. P. Rice et al., "A full-wave HTS flux pump using a feedback control system," *Superconductivity*, vol. 8, no. 4, 2023, Art. no. 100064.

[24] C. Li et al., "A HTS flux pump simulation methodology based on the electrical circuit," *IEEE Trans. Appl. Supercond.*, vol. 30, no. 4, Jun. 2020, Art. no. 4702905.

[25] J. Geng and T. A. Coombs, "Modeling methodology for a HTS flux pump using a 2D H-formulation," *Supercond. Sci. Technol.*, vol. 31, no. 12, 2018, Art. no. 125015.

[26] C. Li, G. Li, Y. Xin, and B. Li, "Modelling methodology for the transformer-rectifier flux pump considering electromagnetic and thermal coupling," *Supercond. Sci. Technol.*, vol. 37, no. 1, 2024, Art. no. 015002.

[27] J. M. Brooks, M. D. Ainslie, Z. Jiang, A. E. Pantoja, R. A. Badcock, and C. W. Bumby, "The transient voltage response of ReBCO coated conductors exhibiting dynamic resistance," *Supercond. Sci. Technol.*, vol. 33, no. 3, 2020, Art. no. 035007.

[28] Z. Jiang et al., "The dynamic resistance of YBCO coated conductor wire: Effect of DC current magnitude and applied field orientation," *Supercond. Sci. Technol.*, vol. 31, no. 3, 2018, Art. no. 035002.

[29] W. Wang and T. Coombs, "Macroscopic magnetic coupling effect: The physical origination of a high-temperature superconducting flux pump," *Phys. Rev. Appl.*, vol. 9, no. 4, 2018, Art. no. 044022.

[30] C. Li, Y. Xing, Y. Xin, B. Li, and F. Grilli, "Time-dependent development of dynamic resistance voltage of superconducting tape considering heat accumulation," *Superconductivity*, vol. 8, 2023, Art. no. 100066.

[31] M. P. Oomen, "Dynamic resistance in a slab-like superconductor with Jc (B) dependence," *Supercond. Sci. Technol.*, vol. 12, pp. 382–387, 1999.